

equilibrium: Zinc in GaAs," *Phys. Rev.* **131**, 1548–1551 (1963).

<sup>9</sup>J. Crank, *Mathematics of Diffusion* (Clarendon, Oxford, 1986).

<sup>10</sup>E. D. Jones, "Measurement of the diffusion of group III elements into cadmium sulphide," Ph.D. thesis, University of Warwick, UK, 1977.

<sup>11</sup>E. D. Jones, "Measurement of the self-diffusion of cadmium into cadmium sulphide using radiotracer techniques," *J. Phys. Chem Solids* **33**, 2063–2069 (1972).

<sup>12</sup>W. Albers, *Physical Chemistry of Defects: Physics and Chemistry of II–VI Compounds*, edited by M. Aven and J. S. Prenner (North-Holland, Amsterdam, 1967).

<sup>13</sup>W. Van Gool, *Principles of Defect Chemistry of Crystalline Solids* (Academic, London, 1966).

<sup>14</sup>E. D. Jones and H. Mykura, "Diffusion of indium into cadmium sulphide," *J. Phys. Chem. Solids* **39**, 11–18 (1978).

## Data analysis in the undergraduate nuclear laboratory

Byron Curry,<sup>a)</sup> Dave Riggins,<sup>a)</sup> and P. B. Siegel

*Physics Department, California State Polytechnic University, Pomona, Pomona, California 91768*

(Received 21 March 1994; accepted 24 June 1994)

Experiments for introducing data analysis techniques in the undergraduate nuclear laboratory are presented. In particular, data from gamma spectroscopy using NaI detectors are ideal for teaching curve fitting and chi-square analysis. An experiment well suited for error analysis is the measurement of the half-life of a radioisotope, since the uncertainties are primarily statistical and can be determined by a well-defined procedure. All software used in our experiments was written by students as special projects. © 1995 American Association of Physics Teachers.

### I. INTRODUCTION

Experiments in nuclear physics that can be performed by undergraduate physics students have been discussed in many books and articles.<sup>1–5</sup> These include the statistics of nuclear decay, measuring alpha, beta, and gamma spectra of radioactive isotopes, and extracting half-lives and other properties of the decay. The main emphasis in these experiments is on observing and measuring different nuclear processes. Since personal computers are now widely available in the laboratory, these experiments also provide an ideal opportunity to introduce curve fitting methods and computer programming into the curriculum. NaI detectors, which are common in student laboratories, have very good characteristics for curve fitting applications: the gamma-ray photopeaks are nearly perfect Gaussian functions (see Fig. 1). In this article we discuss some experiments used in our class in which we instruct the students in chi-square analyses.

Peak fitting is a fairly standard technique, and there is commercial software available for the student laboratory<sup>6</sup> which will extract relevant information from the data. However, since curve-fitting algorithms are not complicated, students can write a program to do the fitting as a special project. Besides giving the student the experience of writing a program to be used in future classes, you can tailor the program to your own needs, and the students in the laboratory class can look at the source code to see how the algorithm is translated into a computer code. Also, when the student will use commercial software in the future to fit data, she or he will have a better understanding of how it works. In our case, the code was written to include a method of determining the uncertainty of all the fitted parameters and the area under the photopeak. With a well-defined statistical uncertainty, chi-square analysis can be properly applied. In our lab we use a chi-square analysis to determine half-lives, gamma attenuation coefficients, and uncertainties in these quantities.

We will first discuss the curve fitting methods we used, and describe some experiments in which single and double peaks are fit. We also discuss how chi-square minimization techniques can be used to determine the half-life and uncertainty of radioisotopes.

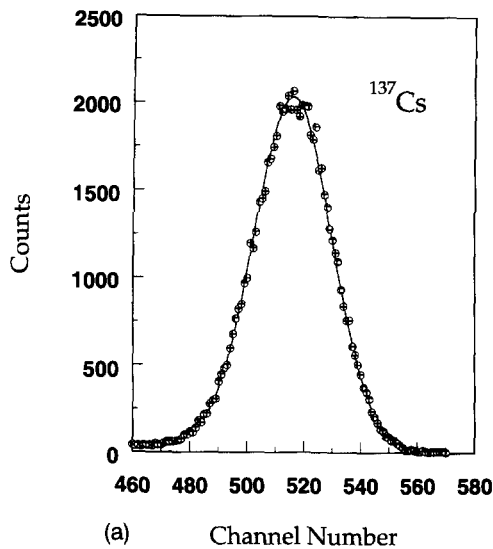
### II. CURVE FITTING METHOD

We will limit our discussion to the fitting of gamma photopeaks obtained from a NaI detector. Most of our detectors consist of a 1–1/2 in. NaI crystal attached to a photomultiplier tube, with the signal input into an amplifier. The amplifier output is read by a PC-based MCA card supplied by the manufacturer.<sup>7</sup> First the manufacturer's acquisition software is used to collect the data. Then the user exits this software to DOS, and the student written program is run which reads the data from the computer's memory. A plot of the counts versus channel number is displayed, and the student decides which peak (or peaks) to fit. Standard techniques for fitting the photopeaks are employed which use a Gaussian function plus background, with three parameters for the Gaussian and two for the background. A best fit is found by varying the five parameters  $x_j$  ( $j=1-5$ ) and minimizing the chi-square function:

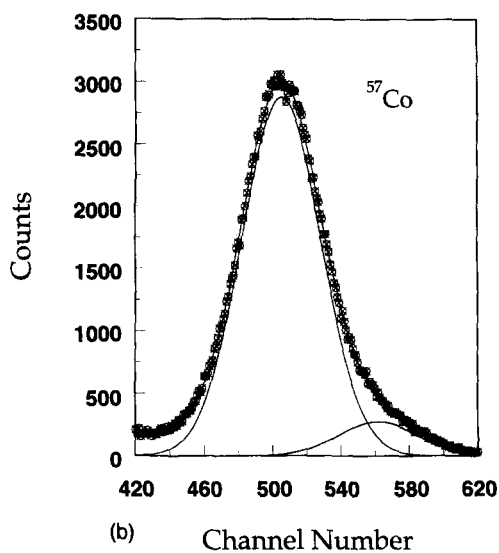
$$\chi^2 = \sum_i \left( \frac{x_3 e^{-[(i-x_1)/x_2]^2} + \text{bkrd}(x_4, x_5, i) - C(i)}{\sqrt{C(i)}} \right)^2, \quad (1)$$

where  $C(i)$  is the number of counts in channel number  $i$ , and  $\text{bkrd}(x_4, x_5, i)$  represents the background.

Different functions for the background were tried, and we found that a good choice was to use a flat plateau before the peak connected by a straight line to a flat plateau after the



(a) Channel Number



(b) Channel Number

Fig. 1. Experimental data along with fitted Gaussian plus background for single and double photopeak fits. (a) The single photopeak fit of  $^{137}\text{Cs}$  demonstrates how well the data is fitted by a Gaussian function. (b) The double photopeak of  $^{57}\text{Co}$  is shown along with the individual Gaussian peaks with the background removed. These common isotopes demonstrate to the students the capabilities of curve fitting.

peak. The plateau before the peak ends at  $x_1 - 2x_2$ , and the plateau after the peak starts at  $x_1 + 2x_2$ . The motivation for this choice is made by noticing that for most of the photopeaks used in the student laboratory, the spectrum just to the right and left of the photopeak is flat and of different heights. Explicitly, the background function was taken to be:

$$\text{bkrd}(x_4, x_5, i) = \begin{cases} x_4 & \text{if } i \leq x_1 - 2x_2 \\ x_4 - \frac{(x_4 - x_5)(i - x_1 + 2x_2)}{4x_2} & \text{if } x_1 - 2x_2 \leq i \leq x_1 + 2x_2 \\ x_5 & \text{if } i \geq x_1 + 2x_2 \end{cases} \quad (2)$$

A graph of this function is shown in Fig. 2. The values of  $x_4$  and  $x_5$  will depend on the photopeak being fitted, but generally  $x_5$  is very small as in Fig. 1. An exception is the 511 keV

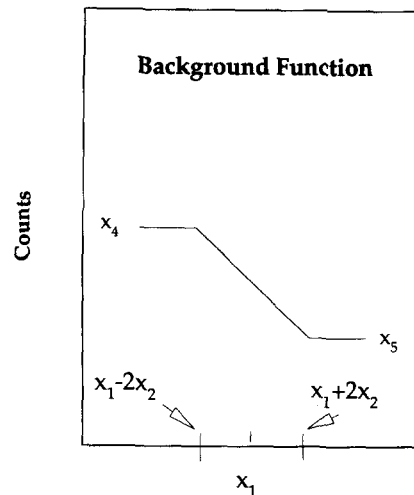


Fig. 2. A graph of the background function for the photopeak fit. The height of the plateau before the peak is  $x_4$  and ends at  $x_1 - 2x_2$ . The plateau after the peak has a height of  $x_5$  and starts at  $x_1 + 2x_2$ . A straight line connects the two plateaus.

photopeak of  $^{22}\text{Na}$ , where Compton scattering from the 1275 keV peak produces a large plateau,  $x_5$ , after the 511 keV peak. Even in this case the background function of Eq. (2) works extremely well, and excellent fits are found with typical values of  $x_4$  being 0.05 and  $x_5$  being 0.03 times the peak height  $x_3$ .

We investigated two different searches for the best fit, a grid search and a gradient search, which were written by students as part of their senior project requirement. The grid search proved to be the best to use since it is conceptually easy for the laboratory students to understand and it runs fast enough. Using an IBM-compatible 386/25 MHz computer with a coprocessor requires less than a second for one run through the five parameters. The grid search method works well when the order of the search is:  $x_1, x_3, x_2, x_4, x_5$ .

The students designed the programs to have just the right user friendliness. The five parameters are initially varied manually by pressing keys to get a close fit to the data. Then a "search key" is pressed to carry out one run of the grid search, and an updated value for  $\chi^2$  is printed on the screen. The search key is repeatedly pressed to do more runs of the grid search until the chi-square function has reached a minimum,  $\chi_{\min}^2$ . This type of interfacing allows the students to get a feeling for what is happening in the search for the minimum and is not simply a "black box" which gives an answer.<sup>8</sup>

In addition to finding the five parameters for the best fit, it is very important to estimate their uncertainties. Since our best-fit values are the result of a search along the  $\chi^2$  hypersurface, there is no simple analytical form for the uncertainties.<sup>9</sup> As discussed in Ref. 9, the uncertainties in the five parameters can be found by examining when the chi-square function increases by one unit. As each parameter is varied from its best-fit value, a search is done on the other four to minimize  $\chi^2$ . For example, to find the uncertainty in the peak center  $x_1$ , the student changes  $x_1$  from its minimum value. Then with this value of  $x_1$  fixed, a search is done on the other four parameters until the  $\chi^2$  function is minimized. Varying  $x_1$  until  $\chi^2$  increases to  $\chi_{\min}^2 + 1$  will give the statis-

tical uncertainty of this parameter. To find the uncertainty in the area under the photopeak, the area is changed from its value at  $\chi_{\min}^2$ . A search is done on the five parameters, while keeping the area constant, to minimize the  $\chi^2$  function. The same procedure of examining when  $\chi^2$  increases by one unit will give the statistical uncertainty in the area. The students can also vary the window of the fit to see how sensitive the fit is to the background function.

Examples of fitted photopeaks are shown in Fig. 1. In Fig. 1(a), the single peak is the photopeak from  $^{137}\text{Cs}$ . The data are fit extremely well with a Gaussian function: the  $\chi^2$  per data point is only 1.3 with a peak height of 2055 counts. To give a rough idea of the uncertainties in such a fit, the peak center is  $515.9 \pm 0.1$ , the standard deviation  $19.35 \pm 0.07$ , and the area  $69040 \pm 274$  counts. We note that an approximate measure of the uncertainty of the area, the square root of the area plus the square root of the background under the peak, is 311 counts. This difference in uncertainties is greater if the counts under the photopeak are smaller. Figure 1(b) displays a double photopeak from the common isotope  $^{57}\text{Co}$ . After failing to obtain a fit with a single peak, the students discover the hidden peak. The  $\chi^2$  per data point for this fit is 0.99 with a peak height of 3055 counts.

### III. SOME LABORATORY EXPERIMENTS

#### A. Half-life of radioisotopes

One of the most suitable experiments for a chi-square analysis is the determination of the half-life of a radioisotope. For this analysis we use the  $^{64}\text{Cu}$  isotope. We make use of our neutron howitzer<sup>3</sup> and the experiment becomes a group activity with the students standing shifts throughout the day. The students are given the task of finding the half-life of  $^{64}\text{Cu}$  and the uncertainty in their measurements. A pure block of copper is placed near our  $^{252}\text{Cf}$  neutron source, and  $^{63}\text{Cu}$  is activated to form  $^{64}\text{Cu}$ . Since  $^{64}\text{Cu}$  has a half-life of around 12 h, the students stand shifts taking a 5 min “live time” count every hour throughout the day. Over the next two days more 5 min counts are taken. The data from a recent laboratory class is listed in Table I. The uncertainty in the counts under the photopeak was determined by the  $\chi_{\min}^2 + 1$  method discussed above.

A common classroom method for determining the half-life of an isotope is to have the students graph the activity versus time on semilog paper, and then do an unweighted linear least-square fit to obtain the slope. Many calculators have this linear regression algorithm built in. A graph of the data of Table I with a linear fit is shown in Fig. 3. This method is simple and gives a good estimate for the slope. However it is only an approximation and is not suited for obtaining the slope's uncertainty. This is because the data are related exponentially, and consequently the errors of the logarithm do not have statistical significance in a  $\chi^2$  sense. It is more appropriate to use a chi-square minimization procedure on the data and its uncertainties, and not on the logarithm of the data.<sup>9</sup> The data of the  $^{64}\text{Cu}$  decay are well suited for this application.

There is discussion in the literature as to the proper chi-square function to use if the variables are not related linearly and if both variables have uncertainties.<sup>10-12</sup> We follow Ref. 10 and use the chi-square function

$$S = \sum_i^n \left( \frac{y_i - f(x_i)}{\delta_i} \right)^2, \quad (3)$$

Table I. Data from  $^{64}\text{Cu}$  decay. Counts under the 511 keV photopeak, for a 5 min count, are listed as a function of the time in hours.

Time	Counts under the photopeak
0	16744 ± 169
1	15596 ± 156
2	15120 ± 159
3	14325 ± 156
4	13723 ± 140
5	12788 ± 138
6	12141 ± 138
7	11277 ± 141
8	10949 ± 134
9	10174 ± 128
25	4317 ± 92
26	4181 ± 89
27	3784 ± 79
29	3454 ± 84
30	3184 ± 77
31	3177 ± 80
32	2910 ± 73
33	2766 ± 77
34	2598 ± 71
49	1274 ± 62
50	1113 ± 55

where

$$\delta_i^2 = \left( \frac{df}{dx_i} \right)^2 (\delta x_i)^2 + (\delta y_i)^2,$$

and  $f(x_i)$  is the fitting function. Since we expect an exponential relationship between activity and time,

$$A(t) = A_0 e^{-\lambda t},$$

an appropriate chi-square function for exponential decay is

$$S(A_0, \lambda) = \sum_i^n \frac{A_i - A_0 e^{-\lambda t_i}}{(\lambda \delta t_i A_i)^2 + (\delta A_i)^2}. \quad (4)$$

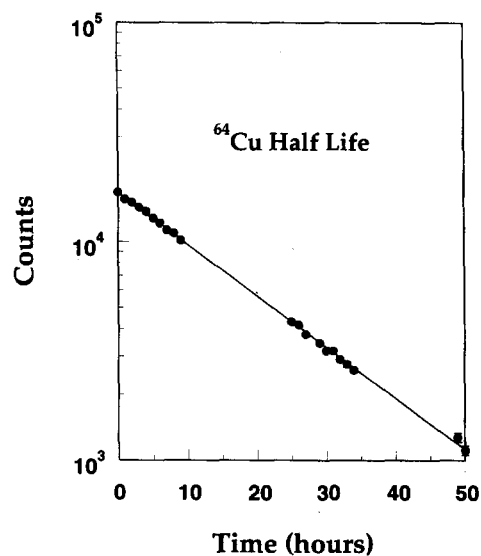


Fig. 3. A semilog graph of the  $^{64}\text{Cu}$  decay data of Table I. The slope, determined by linear regression, gives a half-life of 12.85 h. Except for the last two points, the error bars are smaller than the dots.

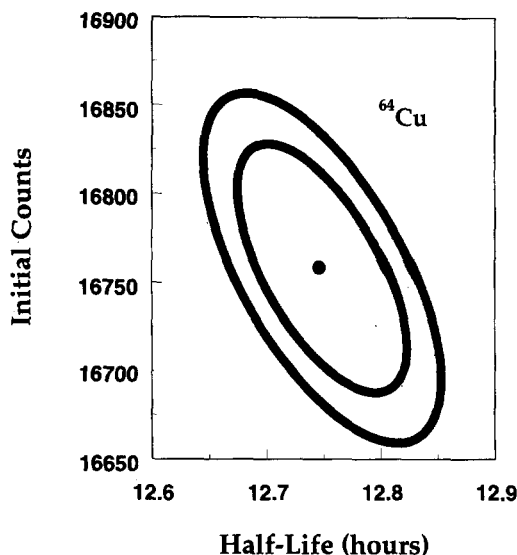


Fig. 4. Equal  $\chi^2$  ovals are plotted in the  $A_0$ –(half-life) plane for the  $^{64}\text{Cu}$  half-life experiment. The point in the middle is  $\chi_{\min}^2$ . Points on the inner oval are the values of  $A_0$  and half-life for which the  $\chi^2$  function is equal to  $\chi_{\min}^2+1$ . The outer oval corresponds to  $\chi_{\min}^2+2$ . The data used to calculate the ovals are from Table I.

In this equation  $A_i$  corresponds to the experimental counts at time  $t_i$ , with uncertainties  $\delta A_i$  and  $\delta t_i$ , respectively.

As a senior project, one of our students wrote a computer program to search on the variables  $A_0$  and  $\lambda$  so as to minimize the chi-square function  $S$ .<sup>8</sup> The starting point of the search was determined from the simple formula for the linear least-square fit of the logarithm of the activity versus time. We found that the best searching procedure was to alternate between a grid and a gradient search. The complementary nature of these two methods gave a very rapid convergence to the minimum value. After finding the minimum chi-square, the program plots ovals of  $\chi_{\min}^2+1$  and  $\chi_{\min}^2+2$  in the  $A_0$ – $\lambda$  plane. In Fig. 4 we show the results from the data of Table I, where we plot the half-life on the  $x$  axis. The program assists the student in determining the bounds of the  $\chi_{\min}^2+1$  oval, and hence the statistical uncertainties of the parameters  $A_0$  and  $\lambda$ . It is also instructive for the students to examine the  $\chi^2$  ovals in the parameter space to see the interplay of the variables in the fit. As seen in Fig. 4, there is a weak dependence of  $\chi^2$  for an increase in the half-life with a corresponding decrease of  $A_0$ . This technique provides an unambiguous method for determining the uncertainty in the half-life of  $^{64}\text{Cu}$ . It also introduces the students to chi-square techniques and the limitations of a linear least-square fit. The student laboratory data of Table I gave a value of  $12.74 \pm 0.06$  h. The linear least-square (linear regression) fit gave a similar value for the half-life of 12.85 h, but the uncertainty could not be obtained. Note that the fit using linear regression falls outside the errors of the  $\chi^2$  fit! The value published in Ref. 13 is 12.701 h.

One of the most common half-life experiments done in the laboratory is the “Cesium Cow” experiment in which  $^{137}\text{Ba}$  is extracted from  $^{137}\text{Cs}$ . If a neutron source is not available, a  $\chi^2$  analysis can also be done with this isotope. The short 2.55 min half-life allows the students to complete the experiment in one lab period, but the students will have to rush to save the data for a meaningful analysis. We have done this experi-

ment counting 30 s of live time every minute. The students have about 20 s to save the data before counting again. Even though the counting time is not small compared to the half-life, the analysis will still be valid if the counting time is the same for each time interval. This is because the effective time of the counting rates will be exactly 1 min apart. In practice, however, there is dead time, and in our case the “real time” varied from 32 to 31 s during the experiment, so the effective time of the counts varied slightly from one minute to the next. Doing the experiment with  $^{64}\text{Cu}$  eliminates this problem. Curve-fitting the photopeak and doing a  $\chi^2$  analysis for the half-life of  $^{137}\text{Ba}$  yielded a value of  $2.55 \pm 0.05$  min in a recent run.

Another option is to do the  $^{137}\text{Ba}$  half-life measurement with a Geiger counter. In this case, the students can still do a  $\chi^2$  analysis for the half-life. The uncertainty of the counts can be approximated as the square root of the counts plus the square root of the background. In a recent experiment we obtained a half-life of  $2.51 \pm 0.04$  min.

An advantage of the half-life experiments is that the main uncertainties are statistical, and that these can be estimated using a well-defined method. There are very few systematic uncertainties since the sample remains in the same position relative to the detector throughout the experiment. The uncertainty in the counting time is perhaps the largest unknown. This is controlled by the MCA card, and is expected to be accurate since it is driven by a crystal. Thus, the student can trace the uncertainties from the fitting of the photopeaks to the chi-square fit of the exponential decay. This analysis parallels that done in many experiments in nuclear and particle physics, and is one of the few examples in the undergraduate curriculum where uncertainties can be given statistical significance.

## B. Calibration of the MCA

A common experiment in the nuclear lab is one in which the detection system is calibrated. This routine exercise also offers an opportunity to introduce the students to the difficulties involved in obtaining accurate energies of emitted gamma rays. The challenge we give the students is the following: determine the energies of the two gamma photopeaks of  $^{207}\text{Bi}$ , and the uncertainties of your values. As standards, they are given  $^{22}\text{Na}$ ,  $^{137}\text{Cs}$ , and  $^{60}\text{Co}$ .

Using the curve fitting routine, the channel numbers of the center of the photopeaks are easily determined. The uncertainty of the channel number is obtained by using the  $\chi_{\min}^2+1$  method described above. The channel number of the center of the photopeak is the most accurate parameter extracted from the peak fit, and its uncertainty varies from 0.1 for single peak fits to 0.5 for double peak fits. Even by varying the window of the fit, the peak center hardly changes. This is because the photopeak data are so well described by a Gaussian. Since the peak center can be measured with such accuracy, the students can be falsely lead to believe that the energies for  $^{207}\text{Bi}$  can be determined to 4 significant figures with the available equipment. However, the detection system is not exactly linear, and the amplifier gain can vary slightly in time. These two properties will cause the greatest uncertainty in the determination of the unknown energies.

The students discover the nonlinearity of the detection system by comparing the channel numbers of the standard sources with their known energies. For our system, the relation of the channel number to the gamma energy was linear to around 5% for energies up to 1.3 MeV. This is demon-

Table II. Standard sources are compared to test the linearity of the detection system.

Channel number	Calculated energy (keV)	Energy from Ref. 13 (keV)
<sup>22</sup> Na 475.7	511	511.003
<sup>137</sup> Cs 610.2	655.5	661.64
<sup>60</sup> Co 1062.2	1141	1173.210
<sup>22</sup> Na 1155.1	1241	1274.5
<sup>60</sup> Co 1203.7	1293	1332.247

strated in Table II in which we compare our standard sources. In column 1 we list the channel numbers of the photopeaks after an offset of 8 has been subtracted. A linear fit is made to the 511 keV photopeak of <sup>22</sup>Na. Extending this fit out to the 1332 keV photopeak of <sup>60</sup>Co results in a prediction which is 3% low. The students can even determine in which part of the system the nonlinearity is the greatest. By examining the sum peak in <sup>22</sup>Na and accounting for the offset of the MCA, we find that the channel number for the 511 keV peak is  $477.3 \pm 0.1$ , the 1275 keV peak is  $1160.0 \pm 0.5$ , and the sum peak is  $1631.1 \pm 1.0$ . This shows that the amplification of the photomultiplier tube and amplifier is linear to better than 0.5%, demonstrating the nonlinearity of the system to be mainly due to the NaI crystal. In determining the unknown energies, one needs to know the exact relationship between energy and channel number,  $E(i)$ , where  $E$  is the energy of the photopeak and  $i$  is the channel number. With a limited number of standard sources available, there will be an uncertainty in determining this relationship.

The slight change in the amplifier gain can be observed by taking measurements at different times during the laboratory period. During a recent measurement we let the amplifier warm up for 30 min, then took a spectrum of <sup>22</sup>Na every 20 min for 2 h. The channel numbers of both the 511 and the 1275 keV peaks slowly increased in time. For the 511 keV peak, the increase was approximately one channel number per hour, and for the 1275 keV peak roughly two channel numbers per hour. To reduce the effects of the variation in amplifier gain, we have the students take data with two sources at the same time. The energy of the lower peak of <sup>207</sup>Bi lies between the 511 keV <sup>22</sup>Na peak and the <sup>137</sup>Cs photopeak. Thus a spectrum with <sup>22</sup>Na + <sup>207</sup>Bi, with <sup>137</sup>Cs + <sup>207</sup>Bi, and with <sup>137</sup>Cs + <sup>22</sup>Na will allow one to reduce the effects of amplifier instabilities.

Interpolation between the standard energies is another source of uncertainty, since  $E(i)$  is not exactly linear. Assuming  $E(i)$  is a smooth function whose derivatives do not change sign between the two standards, the students can bracket the energy of the unknown by using a linear relationship with the lower energy, and then with the higher energy. They can also try a linear plus quadratic fit, and a line between the lower and higher energy standard can be used as well. We find that with our equipment and the standards given, an uncertainty of around 0.3% of the unknown energy can be obtained. A typical result for the two energies of the photopeaks of <sup>207</sup>Bi were  $568 \pm 2$  keV and  $1063 \pm 2$  keV, which agree with published values.<sup>13</sup>

The purpose of this exercise is to instruct the students in some of the difficulties involved in measuring photopeak energies and obtaining accurate standards. To this extent, inexpensive NaI detectors can be used. It is important to point out that in order to calibrate the detection system accurately and recognize its limitations, one needs to know the uncer-

tainties in determining the center of the photopeaks. Using the  $\chi^2_{\min} + 1$  method, we were able to build this feature into our software. We note that the uncertainty of the peak center is not always available with commercial software.

### C. Other experiments

There are other experiments in the nuclear laboratory which offer an opportunity to introduce data analysis techniques. A common experiment is to determine gamma-ray attenuation coefficients by measuring how the gamma-ray intensity is reduced due to varying amounts of absorbing material. Curve fitting and the chi-square function of Eq. (4) can be used in this experiment in exactly the same way the half-life of <sup>64</sup>Cu was determined in the previous section. By curve fitting the photopeak, the total counts and its uncertainty can be determined. Since the intensity falls off exponentially with absorber thickness, the chi-square analysis can be used to determine the attenuation coefficient and its uncertainty. However, there are more systematic errors in this experiment than in the <sup>64</sup>Cu experiment, and the final uncertainty is not mainly statistical as in the half-life experiment.

Measuring the efficiency of the detector as a function of energy and its uncertainty is another useful student exercise. In our lab the students use the sources <sup>57</sup>Co, <sup>137</sup>Cs, <sup>54</sup>Mn, and <sup>60</sup>Co as calibration standards to measure the detector efficiency for the photopeak energies of these standards for a fixed geometry. The uncertainty of the efficiency is largely a result of the uncertainty of the activity of the source. The students are then given the isotope <sup>22</sup>Na and asked to determine the relative probabilities for the isotope to decay via position emission versus electron conversion. Measuring the counts under the 511 and 1275 keV photopeaks and using their results regarding the detector efficiency, they can determine the branching ratio and its uncertainty. Since there is a large uncertainty in the detector efficiency, the students generally are only able to obtain a lower limit for this branching ratio.

Applying a chi-square error analysis in every experiment in the laboratory course is not necessary. One or two experiments per semester give the student enough instruction in data analysis without distracting from the physics. We have used it in the Compton scattering experiment and in alpha and beta spectroscopy. The energy of the conversion electrons for <sup>207</sup>Bi also offers a nice example where we have used the double peak fit to separate out the  $L$  and  $M$  electron energies.<sup>1</sup>

### IV. CONCLUSIONS

We have described some experiments in which data analysis techniques can be introduced in the undergraduate nuclear laboratory class. Generally, experiments in the nuclear lab are geared toward physics principles. However, since the data are often of statistical nature, it offers an ideal opportunity to introduce analysis techniques in some of the experiments. In addition, the students have an opportunity to write the analysis programs themselves as special projects. Although commercial software is available which perform these tasks, the programs are simple enough to be written by students. In our case, two computer programs were developed by students as senior projects to assist in the analysis. One program is designed to fit peaks with a Gaussian plus a background function. The second program performs a chi-square minimization for a two-parameter fit to data which are

related either linearly or exponentially. Both programs allow the user to easily determine the uncertainties in the fitted parameters. A measurement of the half-life of  $^{64}\text{Cu}$  is an excellent student exercise. It is one of the few undergraduate experiments in which all the uncertainties are easily determined by statistical methods.

## ACKNOWLEDGMENTS

We would like to thank the students in the nuclear physics laboratory class for allowing us to use their data. This project was funded by National Science Foundation ILI Grant No. USE-9152011.

<sup>a</sup>This project was done in partial fulfillment of the Bachelor of Science Degree.

<sup>1</sup>D. Desmarais and J. L. Duggan, "Electron conversion for selected nuclides," *Am. J. Phys.* **59**, 56–62 (1991).

<sup>2</sup>D. Desmarais and J. L. Duggan, "Alpha-particle-induced inner-shell ionization measurements for the undergraduate laboratory," *Am. J. Phys.* **52**, 507–513 (1984).

<sup>3</sup>J. L. DuBard and A. Gambhir, "Dust off the neutron howitzer to teach nuclear physics," *Am. J. Phys.* **62**, 255–257 (1994).

<sup>4</sup>M. Mildebrath and S. Cipolla, "Nuclear analyzer-computer interface: An inexpensive digital multichannel analyzer-computer interface for use in the

modern physics laboratory," *Am. J. Phys.* **50**, 667–668 (1982); M. Mildebrath and S. Cipolla, "An improved multichannel analyzer-microcomputer interface," *ibid.* **51**, 1048–1049 (1983).

<sup>5</sup>J. L. Duggan, *Laboratory Investigations in Nuclear Science, Manual LI* (Oxford Instruments, Nuclear Instruments Group, Oak Ridge, 1988).

<sup>6</sup>For example, PEAKFIT from Jandel Scientific offers a variety of Gaussian curve fitting options.

<sup>7</sup>In our laboratory we use two different types of PC based MCA cards: a 1024 channel card by the Nucleus (PCAE), and a 2048 channel card by Ortec. Most of our setups use 1 1/2 in. NaI crystals connected to a model 5010 amplifier from the Nucleus.

<sup>8</sup>The source code for the two student written programs is available from the authors. The curve fitting code is written in PASCAL, and the chi-square minimization code is written in C++.

<sup>9</sup>P. R. Bevington and D. K. Robinson, *Data Reduction and Error Analysis for the Physical Sciences* (McGraw-Hill, New York, 1969).

<sup>10</sup>J. Orear, "Least squares when both variables have uncertainties," *Am. J. Phys.* **50**, 912–916 (1982); "Erratum for 'Least squares when both variables have uncertainties,'" *Am. J. Phys.* **52**, 278 (1984).

<sup>11</sup>B. C. Reed, "Linear least-squares fits with errors in both coordinates," *Am. J. Phys.* **57**, 642–646 (1989).

<sup>12</sup>M. Lybanon, "A better least-squares method when both variables have uncertainties," *Am. J. Phys.* **52**, 22–26 (1984).

<sup>13</sup>The CRC Handbook of Chemistry and Physics lists the half-life of  $^{64}\text{Cu}$  as 12.701 h, and the energies of the two photopeaks of  $^{207}\text{Bi}$  as 569.15 and 1063.10 keV.

## Cyclotron analog applied to the measurement of rolling friction

Ian Edmonds, Nicholas Giannakis, and Chris Henderson

*School of Physics, Queensland University of Technology, P.O. Box 2434, Brisbane, Australia, Q 4000*

(Received 7 February 1994; accepted 14 July 1994)

A simple and inexpensive analog of the cyclotron, ideal for demonstrating the concept of the cyclotron to large classes, is presented. A metal ball, constrained by a centrally directed spring force to follow a circular path over a plane surface, is accelerated by an alternating gravitational force provided manually. A simple method of recording the orbital radius of the ball in the analog provides a sensitive method of measuring the velocity dependent rolling friction force,  $F = a + bv$ . Values of  $a$  and  $b$  for rough and smooth wood surfaces are found and the mechanism by which the losses associated with rolling friction arise is discussed. © 1995 American Association of Physics Teachers.

### I. INTRODUCTION

The cyclotron, developed in the 1930s in the United States by E. O. Lawrence and M. S. Livingston, is used to accelerate protons to energies sufficient to cause transmutation of the elements. From this device, for which Lawrence received a Nobel prize, the synchrocyclotron and the massive present day accelerators were developed. The concept of the cyclotron, the accumulation of small increments of energy by a charged particle constrained by a central force to cycle through an alternating electric field, is one of the more difficult concepts in the introductory physics course. For this reason it is desirable to illustrate the concept with an analog which is simple, visually explanatory, and exciting. Several analogs have been described. In one form,<sup>1</sup> a magnetic analog, a long magnet suspended as a pendulum oscillates through a magnetic field which is reversed manually twice

per cycle until the pendulum acquires a large amplitude. While suitable for class demonstrations, the equipment is elaborate and does not closely simulate the motion of a particle in a cyclotron. In another form,<sup>1</sup> a gravitational analog, a metal ball constrained to move in a spiral cut in a plastic plate is accelerated through the spiral by mechanically driving one-half of the plastic plate alternately above and below the other half at a fixed frequency. While in this apparatus the particle moves on a spiral path, the analogy to a central force is not clear and both the scale and the electromechanical nature of this equipment make it unsuitable for demonstration to large classes.

The analog described here is a gravitational analog of the cyclotron in which a metal ball cycles through an alternating gravitational field while constrained to move in a circular path of ever increasing radius by a central force provided by a spring. The simplicity, manual operation, and scale of the